MASSACHUSETTS INSTITUTE OF TECHNOLOGY

ARTIFICIAL INTELLIGENCE LABORATORY

A.I. Memo No. 467 March 1978

DESTRIPING SATELLITE IMAGES

B. K. P. Horn and R. J. Woodham

Abstract. Before satellite images obtained with multiple image sensors can be used in image analysis, corrections must be introduced for the differences in transfer functions of these sensors. Methods are here presented for obtaining the required information directly from the statistics of the sensor outputs. The assumption is made that the probability distribution of the scene radiance seen by each image sensor is the same. Successful destriping of LANDSAT images is demonstrated.

This report describes research done at the Artificial Intelligence Laboratory of the Massachusetts Institute of Technology. Support for the laboratory's artificial intelligence research is provided in part by the Advanced Research Projects Agency of the Department of Defense under Office of Naval Research contract N00014-75-C-0643.

1. Destriping of images obtained using multiple sensors.

An image sensing device using a single photoelectric sensor which is mechanically scanned across the scene produces outstanding digitized images since sensitivity, resolution and transfer functions are the same for all points in the image. Unfortunately, such a device is limited in speed by the mechanical movement. More importantly, it is limited in speed by the fact that an accurate measurement of scene radiance requires the collection of an adequate number of photons. This explains the preponderance of linear arrays of sensors and area sensors such as vidicons which are otherwise deficient because of geometric distortions, non-uniform response, non-uniform resolution, and so on.

A compromise can be struck, where a small set of sensors is mechanically scanned to collect the image. In the system used aboard LANDSAT, for example, each spectral band is scanned using six sensors at the same time. Thus, six lines of the image are produced during a single sweep of the mirror. On the next sweep the satellite has advanced in its orbit by an amount which allows the same set of sensors to pick up the next six lines of the image [1].

Unfortunately, the sensors do not have identical transfer functions. As a result, images produced in this fashion show undesirable, regular "striping". This effect can be removed if the transfer functions are accurately known, since one could then compute scene radiance from the sensor output using the inverses of these transfer functions. The sensors used in older equipment in particular have time-varying behavior. Photomultipliers, for example, show a drift in both gain and offset (dark current) due to small changes in the material of the dynodes used in the electron multiplier stages and temperature

variations.

If a reference object containing all scene radiances of interest were in the scene, one could recalibrate the sensors continuously. This is difficult to arrange. An alternative is the scanning of a gray wedge placed over a light source at the end of every scan line. This, in fact, is what is done aboard LANDSAT. The results are used to estimate the gains and offsets of the sensors. The digital data produced from the raw satellite signals is corrected using this information [1].

Unfortunately, one finds that the striping effect is not removed in this fashion; the reasons for this are not entirely clear. One cause appears to be the use of the calibration data as a means of adjusting gain and offset so that each sensor is related to its preflight condition. Slight changes in the light source, the gray wedge and the geometry of imaging introduce drifts which are not compensated for. Another reason is related to the fact that photomultipliers are somewhat nonlinear and have a response which depends on their exposure history. Modern devices using solid state photodiodes do not suffer from these problems.

The methods explored here for destriping images are based on the assumption that each sensor is exposed to scene radiances with approximately the same probability distribution. The sensor values can then be modified so that each one is related in the same way to the actual scene radiance. The information required to perform this modification is extracted from statistics of the observed sensor outputs.

2. A simple method for linear transducers.

If the image sensors are linear and time invariant, a simple method can be used to reduce striping. The sensor output, x', can be written as a function of the scene radiance, x, as follows:

$$x' = f(x) = a + b \cdot x$$

Each sensor has its own, fixed values of offset, a, and gain, b. If these are known, the scene radiance can be calculated using the inverse of the transfer function,

$$x = g(x') = (x' - a)/b$$

If this is done for each sensor in turn, striping effects will be removed.

The required constants for each sensor can be determined if a calibration object containing two or more known scene radiance values is available in the scanned scene. If such a calibration object is not available one can estimate the (relative) values of gain and offset using simple statistics of observed sensor values. Each sensor sees a subimage consisting of every nth line (when n sensors are used). The complete image is formed by interlacing these subimages. It seems reasonable to suppose that, for a large enough image, each subimage has approximately the same probability distribution of scene radiance values. One would not expect a particular subimage to contain many more values in a particular range of scene radiances than another subimage.

If this assumption is correct, then the gain and offset constants can be

estimated from the mean and standard deviation of the measured sensor output values. If the mean of the scene radiance is μ and the standard deviation is σ, then the mean of the sensor output will be $\mu' = a + b\,\mu$ and the standard deviation of the sensor output $\sigma' = b\,\sigma$. Then,

$$b = \sigma'/\sigma$$

and

$$a = (\mu'\,\sigma - \mu\,\sigma')/\sigma$$

Clearly, it is not reasonable to assume that one can find the absolute values of the mean and standard deviation of the actual scene radiance. Fortunately, for destriping purposes only relative values are important. That is, one can use the mean and standard deviation of the sensor outputs for the whole image in place of the mean and standard deviation of the scene radiance. Naturally now the results will not be scene radiance values. The striping however will be removed since each subimage now has the same mean and standard deviation, and, if the assumption introduced earlier applies, the same linear relationship to scene radiance.

Note that one can relax the assumption about the relationship of the subimages. Here it is not necessary that they have the same probability distribution of scene radiance, only that their means and standard deviations be the same. This simple method has been applied by some users of LANDSAT data [2,3].

3. Shortcomings of the simple method.

We have found this method to be only partially successful in destriping LANDSAT images. One reason for this may be that out of a range of 128 possible sensor outputs a range of only around 30 values correspond to normal scene radiance values. Low values are not found in short wavelength bands because of light scatter in the air. Conversely, large values correspond to cloud, snow and ice, and scene radiance values of such areas often exceed the highest available sensor output values and so result in clipping. Clipping of sensor values corresponding to low scene radiances also occurs at times in the long wavelength bands due to negative sensor offsets. Both of these nonlinear effects will introduce skew into the calculation of means and standard deviations.

One may alleviate this problem by removing sensor values outside a certain range from consideration. While slightly better results are obtained in this fashion, it is clear that the arbitrarily selected thresholds needed introduce biases of their own. This later effect can be dealt with by eliminating the same fraction of sensor values from the low end of the output of each sensor. Similarly, a fixed fraction of sensor values is removed from the high end.

Even with this refinement, results are not entirely satisfactory. Superficially, it appears that different gains and offsets are appropriate for different scene radiance ranges. That is, the sensor transfer curves are somewhat nonlinear. We thus devised a method which deals with this problem directly.

4. Preliminary considerations.

Consider a random variable X with probability density function p(x). The function p(x) is non-negative and satisfies

$$\int_{-\infty}^{\infty} p(x)\, dx = 1$$

The probability density function p(x) can be estimated from a large number N of observations of the random variable X. If n of these measurements fall in the interval $[x, x + \delta x]$, then n/N tends to $p(x)\,\delta x$ as N becomes very large and δx small (in a fashion which allows $N\,\delta x$, and thus n, to become large also).

The cumulative probability density function P(x) is defined as

$$P(x) = \int_{-\infty}^{x} p(t)\, dt$$

This function is monotonically non-decreasing since p(x) is non-negative. P(x) represents the probability that the random variable X takes on a value less than or equal to x.

Now consider observing the random variable X by means of a transducer with transfer function f(x). Its output can be thought of as a new random variable X', say, with a probability density function p'(x'). This function is related to the probability density function p(x) of the original random variable X, in a fashion which depends on the transfer function x' = f(x). It is easiest to develop this relationship in terms of the cumulative distri-

bution functions P(x) and P'(x') where

$$P'(x') = \int_{-\infty}^{x'} p'(t)\, dt$$

If x' lies in a range R' when x lies in the range R, then clearly,

$$\int_{R'} p'(x')\, dx' = \int_{R} p(x)\, dx$$

Now assume that f(x) is monotonically non-decreasing. Then the range $x \leq x_0$ is mapped into the range $x' \leq f(x_0)$.

$$P'[f(x)] = P(x)$$

As a result one can determine the transfer function f(x) if the cumulative probability density functions P(x) and P'(x) are known and if the latter has an inverse. Then,

$$f(x) = (P')^{-1}\, P(x)$$

If P' is monotonically increasing, the required inverse will exist. Difficulties will be encountered only when P'(x') is constant over a certain range. That is, if $P'(x') = c$ [and hence $p'(x') = 0$] for $x' \in [x_1', x_2']$. Then, if $P(x) = c$, one can say only that $f(x) \in [x_1', x_2']$.

There are two possible causes of this problem. First it may be that f(x)

actually has a discontinuity. In this case, one correctly finds a jump from x'_1 to x'_2 in the solution. The other possibility is more serious. If $p'(x') = 0$ because $p(x) = 0$ [where $x' = f(x)$ as before], then the transfer function $f(x)$ cannot be found in the specified range because, in essence, no inputs are available to test it in this range. The information to recover $f(x)$ there is thus not available.

Note, however, that if the inputs to the transducer are in fact characterized by the given probability density function, then our lack of knowledge of the transfer function in the specified range is of no consequence since no inputs fall in this range anyway.

To calculate scene radiance from sensor values, we actually need the inverse $g(x')$ of the transfer function. This can be found just as easily. If,

$$P'(x') = P\,[g(x')]$$

Then

$$g(x') = P^{-1}\,P'(x')$$

The same considerations regarding the existence of the inverse P^{-1} apply here as those discussed regarding the existence of the inverse $(P')^{-1}$. All these special case problems are avoided if the cumulative probability distribution functions are monotonically increasing.

The method shown here for finding the transfer function of a transducer (or its inverse) is based on the same analysis as that used to design a generator of pseudo-random numbers with a desired probability distribution function

p'(x) when a generator is available which produces pseudo-random numbers with known probability distribution function p(x) [4].

A graphical illustration of the relationships discussed may be found in Figure 1. The dotted line suggests how one may determine the transfer function value, f(x), given a scene radiance value x. Conversely, the same dotted line may be followed in the reverse direction to find the value, g(x'), of the inverse function from a given value of the transducer output x'.

5. Estimation from a finite number of samples.

To apply this method to determine the transfer function of a real transducer, the cumulative probability density functions must be determined from a model of the underlying process generating the random variables or estimated from frequencies of observed occurrence using a finite number of samples. In the latter case an uncertainty will be found in the estimation of the probabilities which will be inversely proportional to the square root of the number of samples falling in a particular interval.

In particular, the sample deviation of the estimate of the cumulative probability P(x) obtained from a total of N measurements is

$$\sigma P = \sqrt{P(1 - P)/N}$$

The following approximate analysis may be helpful: Let σf be the uncertainty in estimating the transfer function, $x' = f(x)$, resulting from the uncertainty σP in estimating P(x), then,

$$P'[f(x) + \sigma f] = P(x) + \sigma P$$

If P'(x') is reasonably well behaved then the left-hand side can be expanded,

$$P'[f(x)] + p'(x')\ \sigma f \simeq P(x) + \sigma P$$

using the fact that p' is the first derivative of P'. Clearly then

$$p'(x')\ \sigma f \simeq \sigma P$$

The uncertainty in estimating the transfer function $x' = f(x)$ is thus highest where $p'(x')$ is small. In fact, we have already shown that $f(x)$ cannot be uniquely determined when $p'(x') = 0$.

One can similarly show that

$$p(x)\ \sigma g \approx \sigma P'$$

where σg is the uncertainty in estimating the inverse transfer function, $x = g(x')$, due to uncertainty σP in estimating $P'(x')$. Not surprisingly, uncertainty in estimating the inverse transfer function is highest where $p(x)$ is small.

The probability density functions $p(x)$ and $p'(x')$ are related by,

$$p(x) = p'(x') \frac{df}{dx} \qquad \text{and} \qquad p'(x') = p(x) \frac{dg}{dx'}$$

when the indicated derivatives exist.

6. Transducer with discrete output values.

Essentially the same method may be used if the transducer produces discrete outputs. Consider, for example, a case where the input range can be broken up into a number of intervals such that

$$f(x) = i \qquad \text{if } x \in [x_i, x_{i+1})$$

The probability density function of the output of the transducer is then discrete and,

$$p'_i = \lim_{\varepsilon \to 0} \int_{x_i}^{x_{i+1} - \varepsilon} p(x)\, dx$$

Clearly, $p'_i \geq 0$ and

$$\sum_{i = -\infty}^{\infty} p'_i = 1$$

The cumulative probability density function can be defined as follows

$$P'_i = \sum_{a = -\infty}^{i} p'_a$$

If $f(x)$ is monotonically non-decreasing, then the same argument applied in the continuous case, leads again to

$$P'_{[f(x)]} = P(x)$$

If P' can be inverted, the transfer function can be found using

$$f(x) = (P')^{-1} P(x)$$

The only difference is that here f(x) is a function from a continuous range to a discrete domain. Naturally, when one finds the inverse of the transfer function, g(x'), using these methods, one has to accept the fact that the actual value of x cannot be recovered, only a range $[x_i, x_{i+1})$.

7. Application to satellite images.

A particular sensor, in a system using n sensors, sees a subimage containing every n^{th} line. To apply the methods developed here one has to assume that each sensor is exposed to scene radiances with similar probability distributions. If the image is large enough, it is very unlikely that one sensor will see substantially fewer or more scene radiances in a particular range. A sensor's properties can then be estimated from the statistics of its outputs.

Since the probability distribution function of the actual scene radiance is not available, only relative adjustments can be made. That is, the probability distribution function of sensor outputs for the whole image is used as a reference. Consequently, application of the inverse functions so determined to each subimage will not produce scene radiances. It will, however, result in an image in which each image gray level is related to the scene radiance in the same way. Thus, striping will have been removed.

A graphical illustration of the method is shown in Figure 2. Note that here both P(x) and P'(x') are discrete. This results in a small problem when the transfer function f(x) is to be found using data from a real image. For perfect data, there always is a value x' for every value x, such that P'(x') = P(x). As indicated by the dotted line in the figure, this may not be the case when the data is obtained from a finite number of samples obtained by different sensors. The best one can do then is to find a value x' such that

$$P'(x') \leq P(x) < P'(x' + 1)$$

Similarly, in determining the inverse transfer function g(x'), one can do no

better than finding a value x such that

$$P(x) \leq P'(x') < P(x + 1)$$

What value should be used in the lookup table for destriping? One might argue that some values should be translated to x, others to (x + 1). If this is done in the appropriate fashion, the histogram of gray levels in the destriped image will equal the histogram of gray levels in the raw image. It is difficult however to decide which points should receive one value and which the other. If the selection is based on a random number generator, additional noise will be introduced. In any case a change smaller than one gray level is usually negligible considering the limitations of radiometric accuracy in the imaging system. The algorithm we employed, arbitrarily uses the smaller value of the two possible ones. Note that the histogram of the destriped image will not be exactly equal to the histogram of the raw image when this is done.

8. Details of the algorithms.

The first step is the determination of a cumulative histogram of sensor values for the whole image as a reference. Let there be H(x) occurrences of sensor outputs less than or equal to x out of a total of N values. Now for the subimage produced by sensor i, one calculates a similar cumulative histogram. Let $H_i(x')$ be the number of sensor outputs less than or equal to x', produced by sensor i, out of a total of N_i values. Here,

$$N = \sum_{i=1}^{n} N_i$$

where n is the number of sensors.

A lookup table g(x') is now constructed by applying the inverse of the function H(x) to $H_i(x')$. This lookup table is then used to modify all the sensor values produced by sensor i. The inverse can be calculated relatively easily since H(x) is a monotonically non-decreasing function. The lookup table value g(x') is the smallest number x such that

$$N_i\ H(x) \leq N\ H_i(x') < N_i\ H(x + 1)$$

This process is repeated for each sensor in turn, until all image values have been modified by the lookup table appropriate to the sensor with which they were measured.

9. Results.

The image used for the illustrations here is a part of LANDSAT-1 image E-1078-09555 taken 1972/October/9. The part used contains 364 lines each of 430 pixels. The worst striping in this case occurred in band 6 (.7μ to .8μ) and band 7 (.8μ to 1.1μ), so the discussion will concentrate on these two. The data transmitted from the spacecraft is pseudo-logarithmically compressed and converted to six bit numbers. On the ground the compression is removed using a lookup table. The result is a seven bit number. Naturally, about half of the possible seven bit numbers never occur in a given subimage. Furthermore, scene radiance corresponding to normal surfaces (Other than ice, snow or cloud) occupy only the lower 25% to 35% of the available range. As a result, the total range of scene radiances of interest corresponds to a very small set of distinct sensor output values. This contributes a little to difficulties in completely removing striping effects.

Comparison of Figure 3, the original band 6 image, with Figure 4, the processed version, shows that the heavy, regular striping is removed by the processing described here. It is instructive to inspect the lookup tables used for each sensor. These are shown as six subfigures in Figure 5. The short horizontal sections in the transfer function correspond to sensor values which never occur as a result of the decompression table lookup. The inverse transfer functions shown in Figure 5 appear to evidence some nonlinearities. This explains why the simple destriping technique described earlier does not do as well.

Comparison of Figure 6, the original band 7 image, with Figure 7, the processed version, shows that the regular striping is removed here as well.

The very light striping remaining in shadow areas amounts to fluctuations of only one or two pixel values, but may be discernable because of the human observer's sensitivity to small differences of reflectance in dark areas. Inspection of the histograms of raw image data reveals uneven intervals in the analog-to-digital convertors used, which contribute to this effect (in fact some codes near major transitions never occur). The relative smoothness of the lookup tables used in destriping this band, shown in Figure 8, is in part due to the fact that no compression and decompression is performed on data for this band; six bit numbers linearly related to sensor output being transmitted directly. The inverse transfer functions shown in Figure 8 appear to be fairly linear, which is probably a result of the linearity of the silicon photodiodes used for this infrared band. One would expect then that the simple destriping method would be fairly successful for this band.

We experienced some difficulties due to the normalization processing performed on the raw LANDSAT data. It may be useful to provide users of LANDSAT tapes optionally with the original data. Preliminary results indicate that slightly better destriping may be possible using the raw image sensor values. It is also unfortunate that areas of high reflectance produce scene radiances which saturate the imaging system. If this was not the case, image sensor outputs corresponding to areas covered by thick clouds could be used in calibration of absolute reflectances as well as in normalization for destriping purposes.

10. Relation to Histogram Normalization Methods.

A number of techniques aimed at the enhancement of images intended for human viewing are based on manipulation of the gray level histogram. Some, for example, transform the histogram into one considered more desirable [5, 6, 7, 8, 9], either flat or "hyperbolic". The suggestion has been made that such techniques may allow for changes in sensor characteristics or scene illumination [6, 8, 10]. Several suggestions have been made regarding the difficulty indicated in Figure 2 relating to the mismatch of two cumulative histograms. One can, for example, increase the apparent fineness of quantization by taking into account the context of each picture cell [7]. If each picture cell has a maximum gray level value m and k neighbors, one may multiply its gray level value by mk and subtract (or add) the sum of the neighboring gray level values. In this way rank-ordering of picture cell values is preserved, while the number of possible gray level values is vastly increased, bringing the distributions closer to those found in the continuous case.

Recent work on matching of images obtained by one sensor at different times is perhaps most closely related to our work here on destriping [10]. This sort of approach has however not yet found much of a following in the remote sensing community [11]. We believe our application of histogram "equalization" to subimages obtained using sensors of a multiple-sensor system is novel.

11. Conclusions.

The following can be accomplished using the method presented here:

1. The effect of differences in the transfer functions of the different sensors is removed. All gray levels are then related in the same way to the original scene radiance values.

2. The overall tone-scale is preserved. That is, the histogram of gray levels of the destriped image is (approximately) the same as the histogram of the raw image. There is no loss in resolution, nor is the noise level increased.

3. The computation requires only two serial passes over the whole image: one to collect the relevant histograms, another to apply the inverse transducer function represented as a simple lookup table.

12. References.

1. LANDSAT Data Users Handbook, NASA Document No. 76SDS4258, Goddard Space Flight Center, Greenbelt, Maryland, September 1976.
2. W. M. Strome & S. S. Vishnubhatla, "A system for improving the radiometric corrections for ERTS-1 MSS data", Paper presented at XXIV Int. Astronautical Congress, Baku, USSR, October 1973.
3. D. S. Sloan & R. Orth, "A self-contained LANDSAT data reception and precision cartographic image production system", Paper presented at the Int. Symp. of Comm. III of the Int. Soc. for Photogrammetry, Graz, Austria, October 3-5 1977.
4. D. E. Knuth, The Art of Computer Programming, Vol. 2, Reading, MA, Addison-Wesley, 1969, pp. 102-103.
5. E. H. Hall, "Almost uniform distributions for computer image enhancement", IEEE Trans. Comput. C-23, 1974, pp. 207-208.
6. R. M. Haralick, "Automatic remote sensor image processing" in Digital Picture Analysis, A. Rosenfeld (ed.), Berlin, Springer, 1976, pp. 12-16.
7. R. A. Hummel, "Histogram modification techniques" Computer Graphics and Image Processing, Vol. 4, 1975, pp. 209-224.
8. A. Rosenfeld & A. C. Kak, Digital Picture Processing, New York, Academic Press, 1976, pp. 173-176.
9. Werner Frei, "Image enhancement by histogram hyperbolization", Computer Graphics and Image Processing, Vol. 6, 1977, pp. 286-294.
10. We-Min Chow & Lawrence T. Kou, "Matching two digital pictures", IBM Research Report RC 6870, November 1977.
11. J. Lintz Jr. & D. S. Simonett (eds.), Remote Sensing of the Environment, Reading, MA, Addison-Wesley, 1976.

13. Figures.

Figure 1. The transfer function, $x' = f(x)$, of a transducer can be found if the cumulative probability distribution functions of its input, x, and its output, x', are known.

Figure 2. When both cumulative probability distribution functions are discrete, there may not be a value of x' so that $P(x') = P(x)$. Some rule must be adopted to deal with this.

Figure 3. Original, unrectified image of band 6 (.7μ to .8μ) output of LANDSAT. Notice the heavy, regular striping.

Figure 4. Destriped image of band 6 output.

Figure 5. The destriping lookup tables for band 6 -- inverse transfer functions for the six image sensors. The nonlinearities of the transducers are apparent.

Figure 6. Original, unrectified image of band 7 (.8μ to 1.1μ) output of LANDSAT. Notice regular striping.

Figure 7. Destriped image of band 7 output.

Figure 8. The destriping lookup tables for band 7 -- inverse transfer functions for the six image sensors. These transducers appear to be fairly linear, differing mostly only as regards gain or amplification.

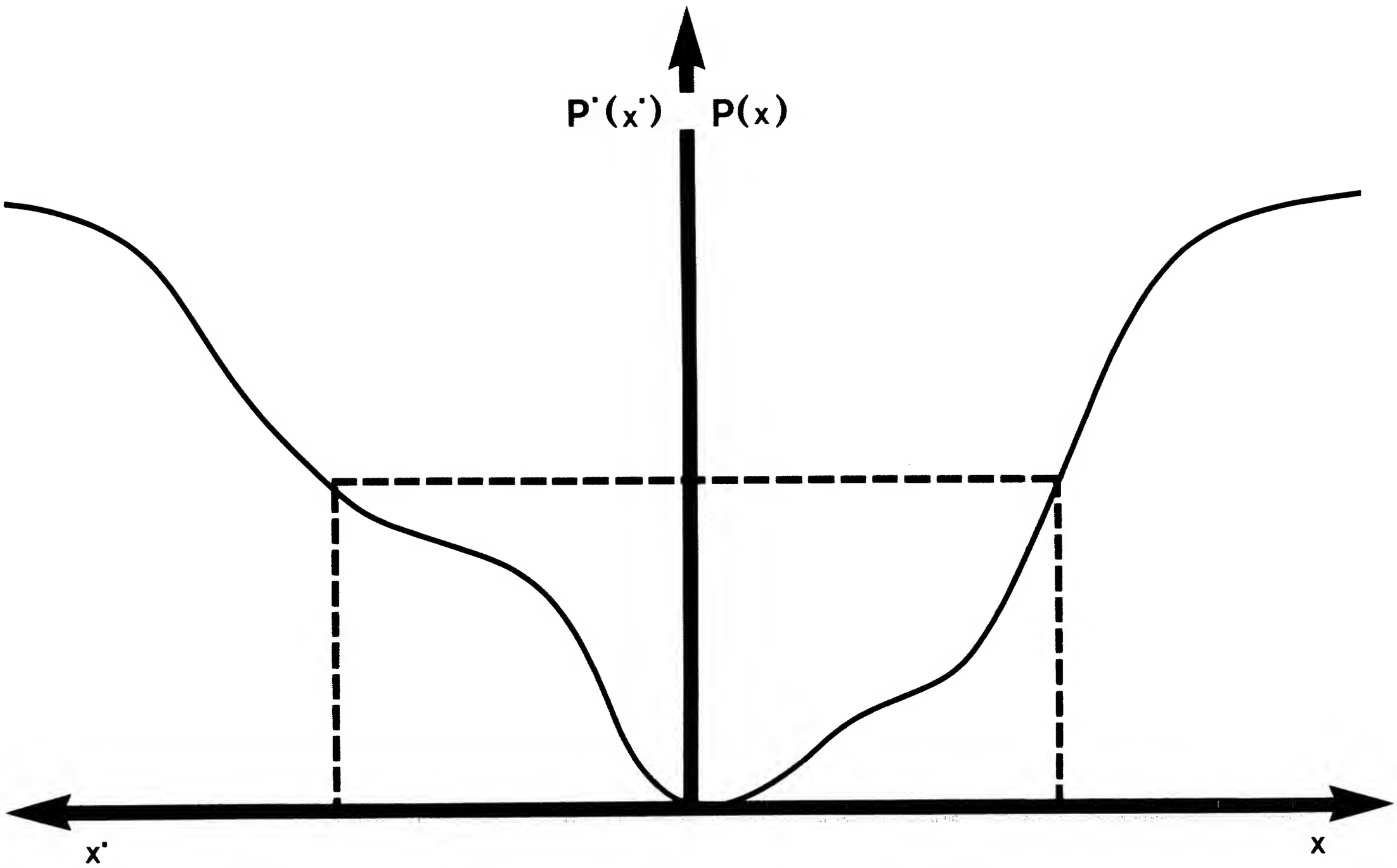

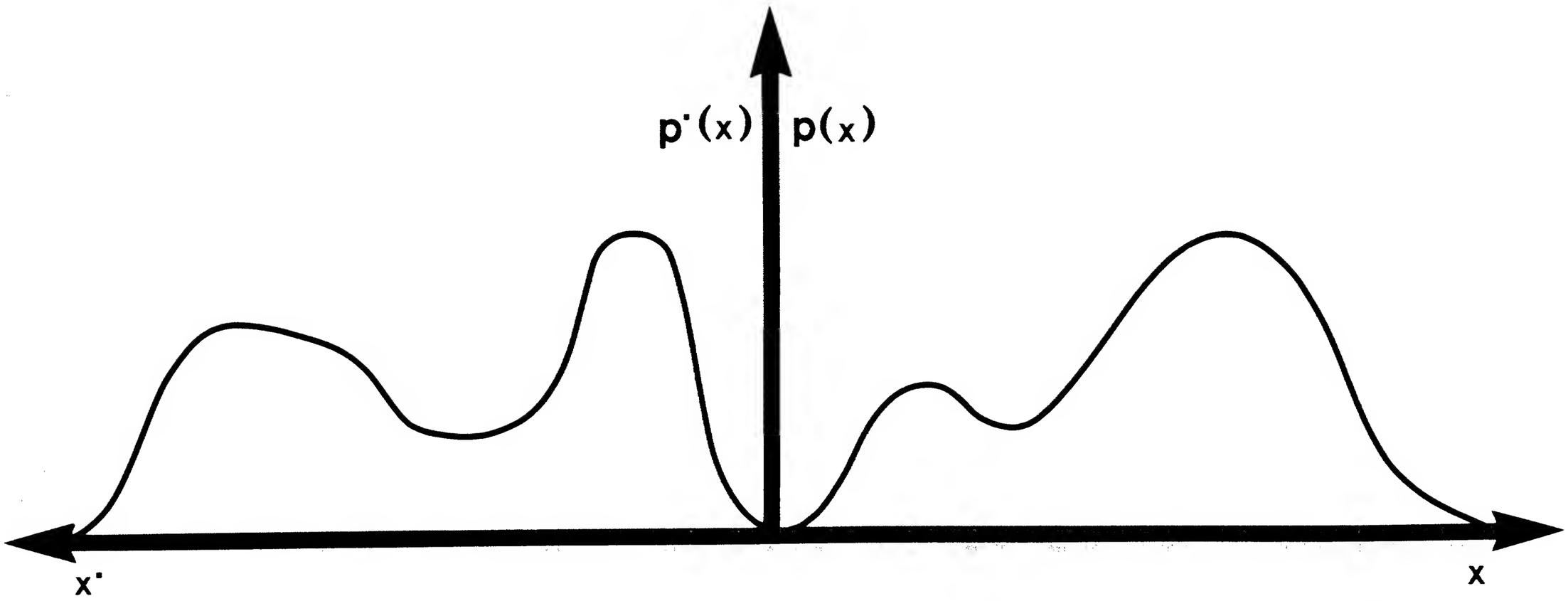

FIGURE 1

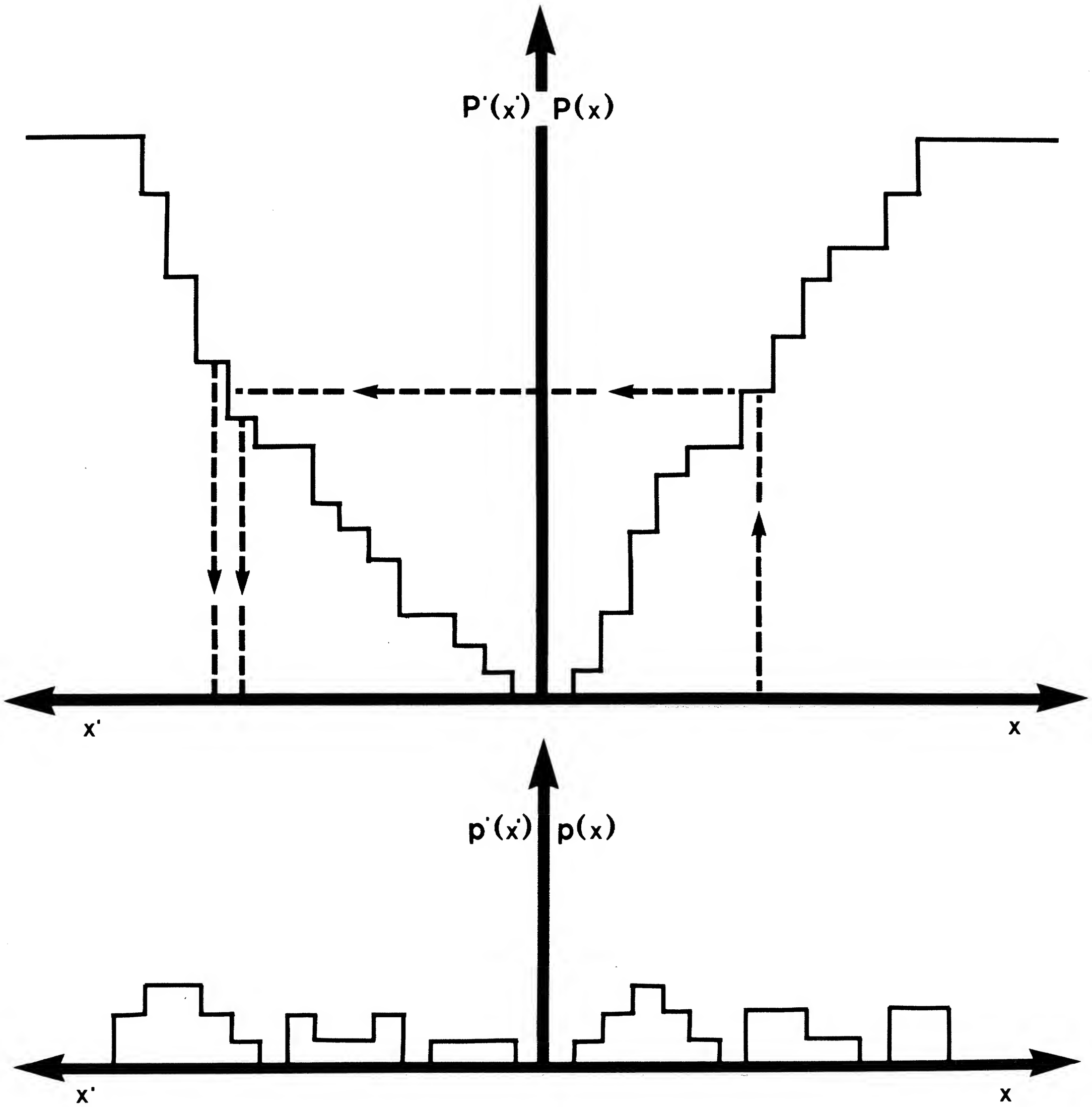

FIGURE 2

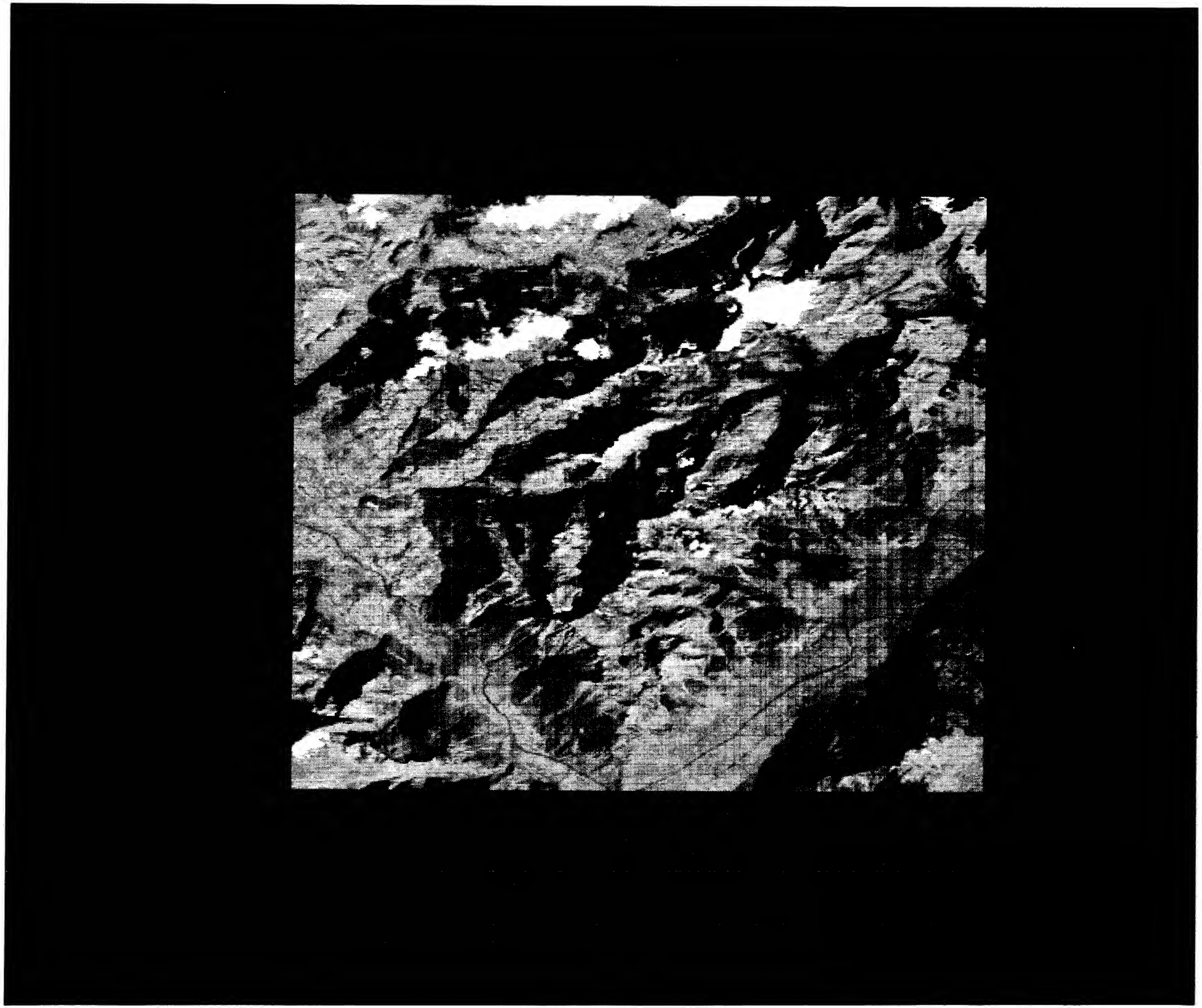

Fig 3

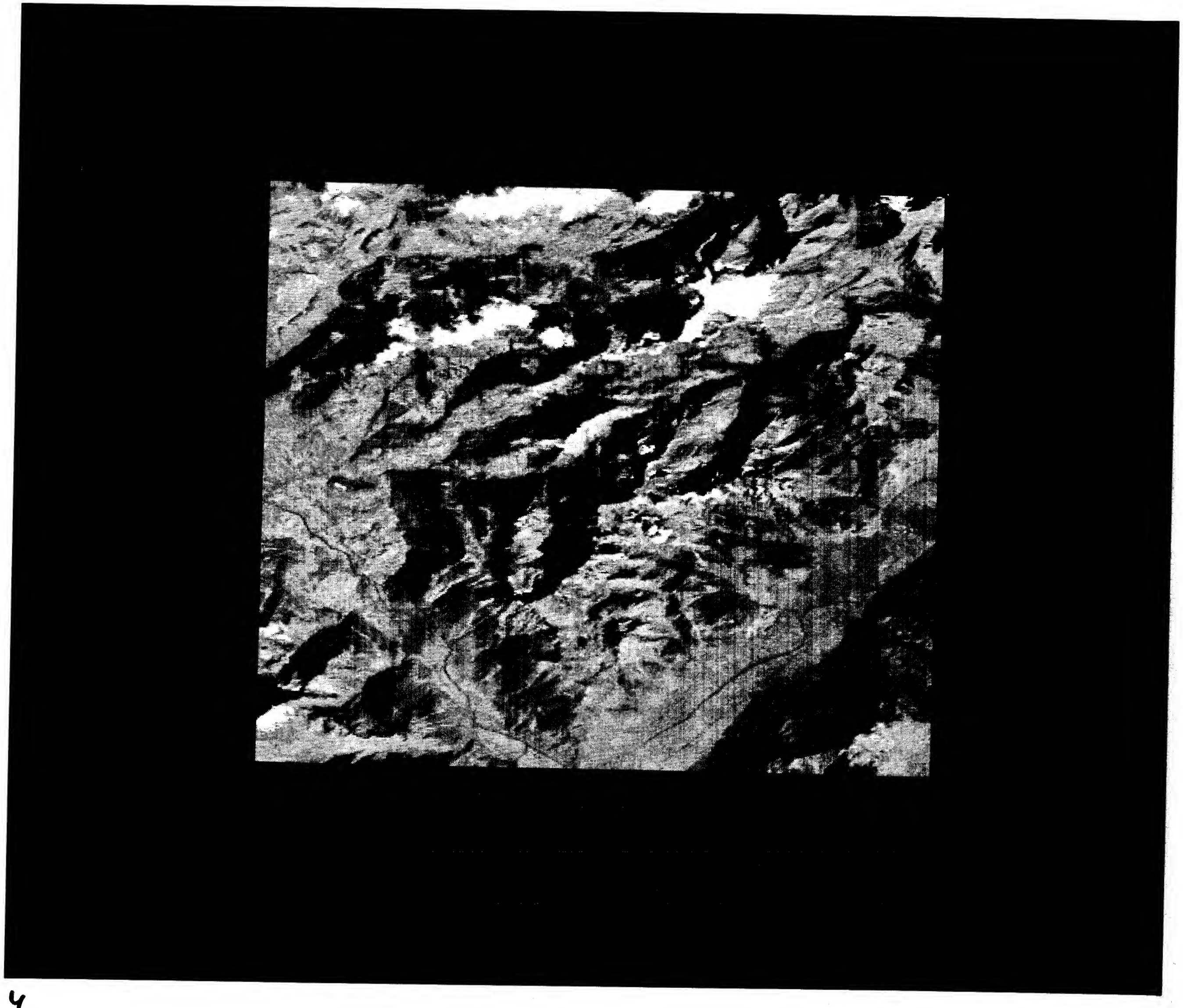

Fig 4

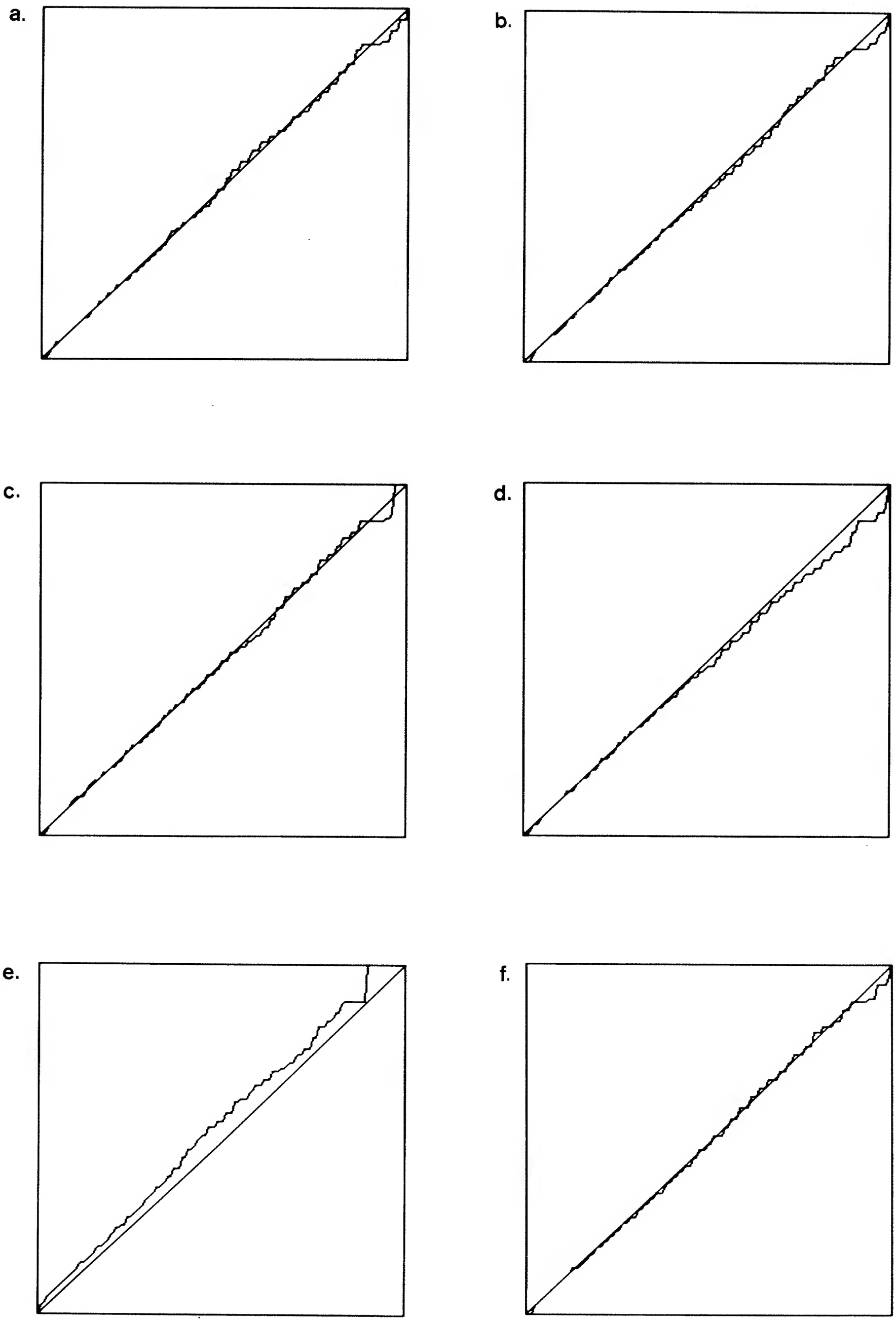

FIGURE 5

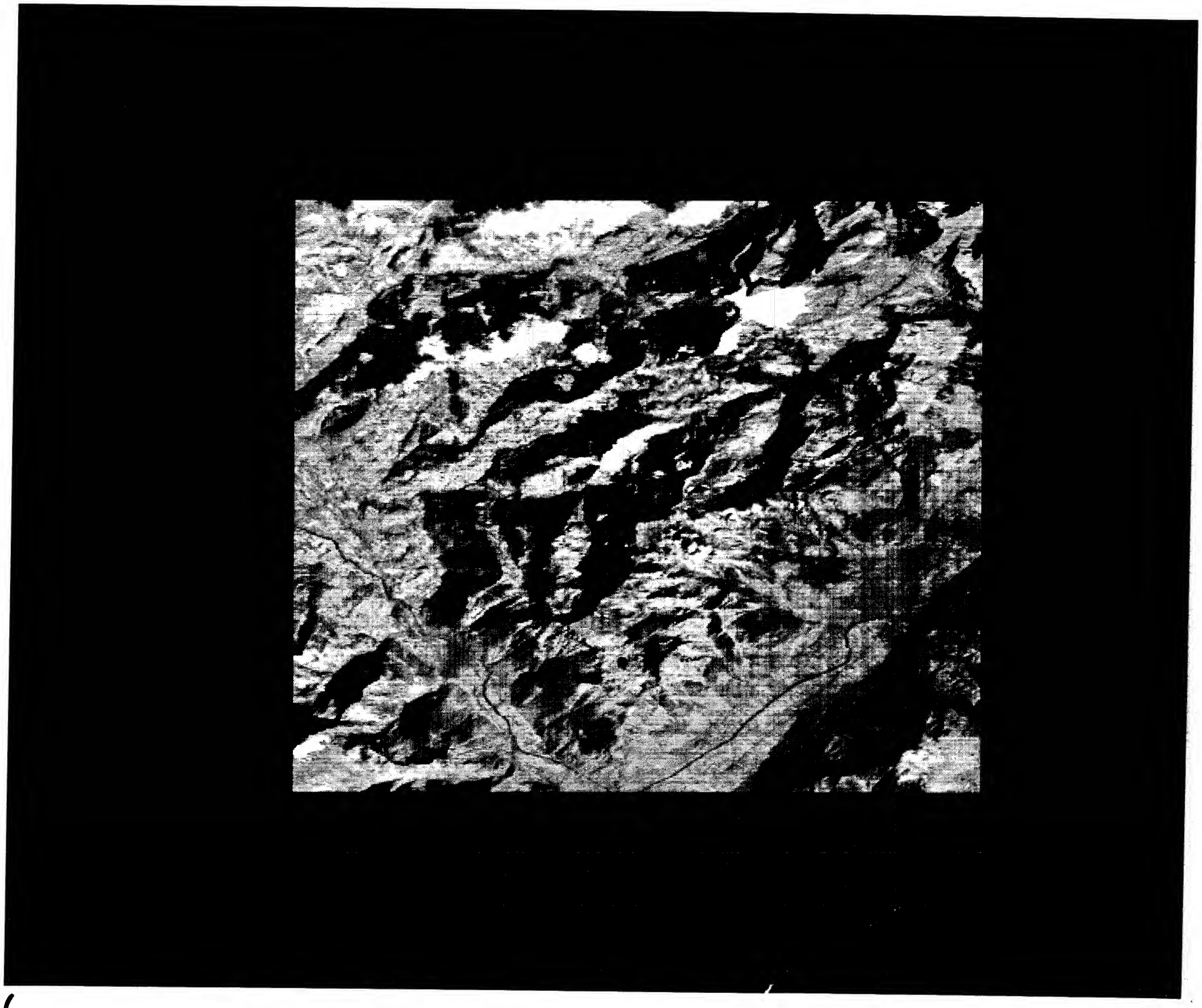

Fig 6

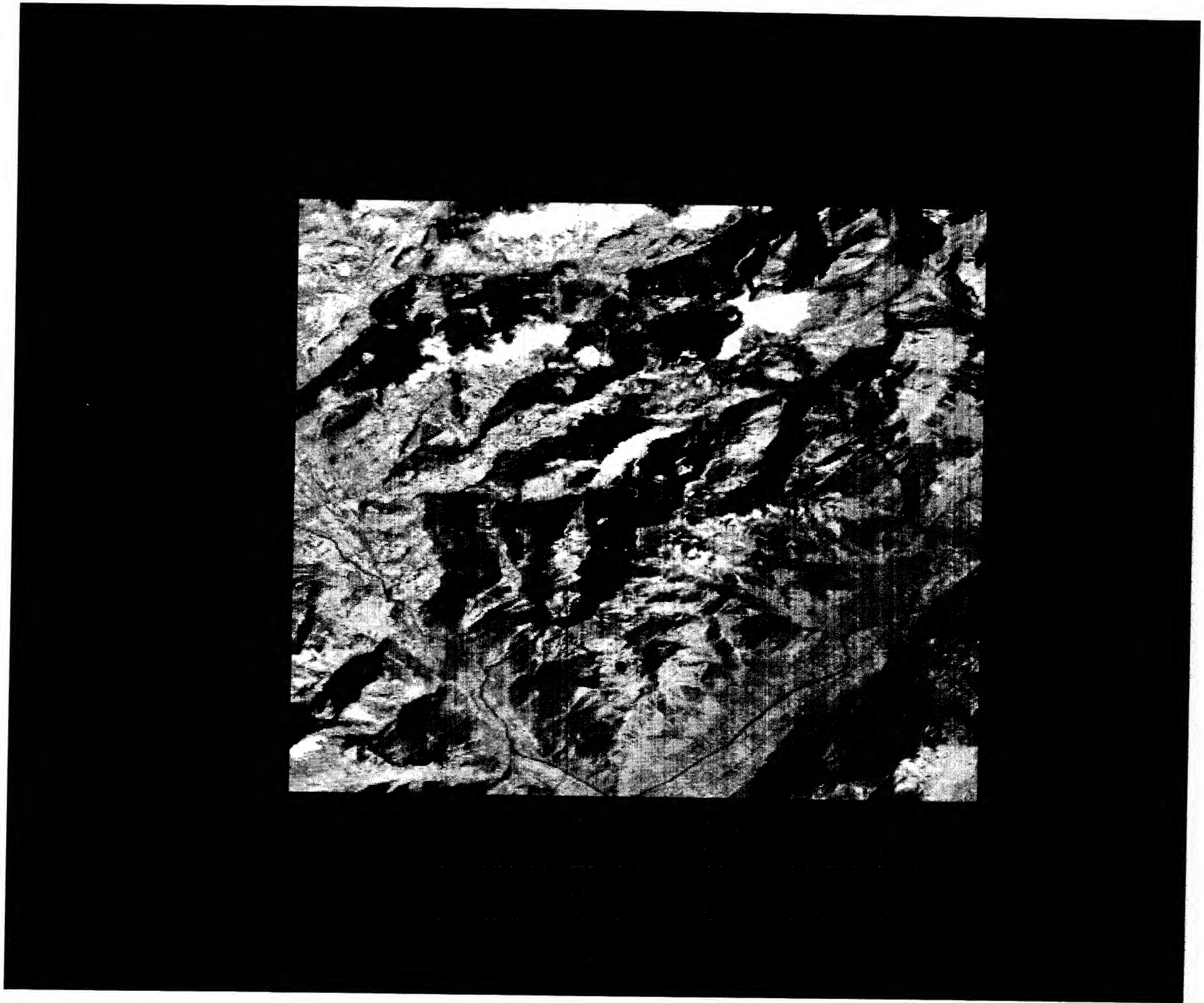

Fig 7

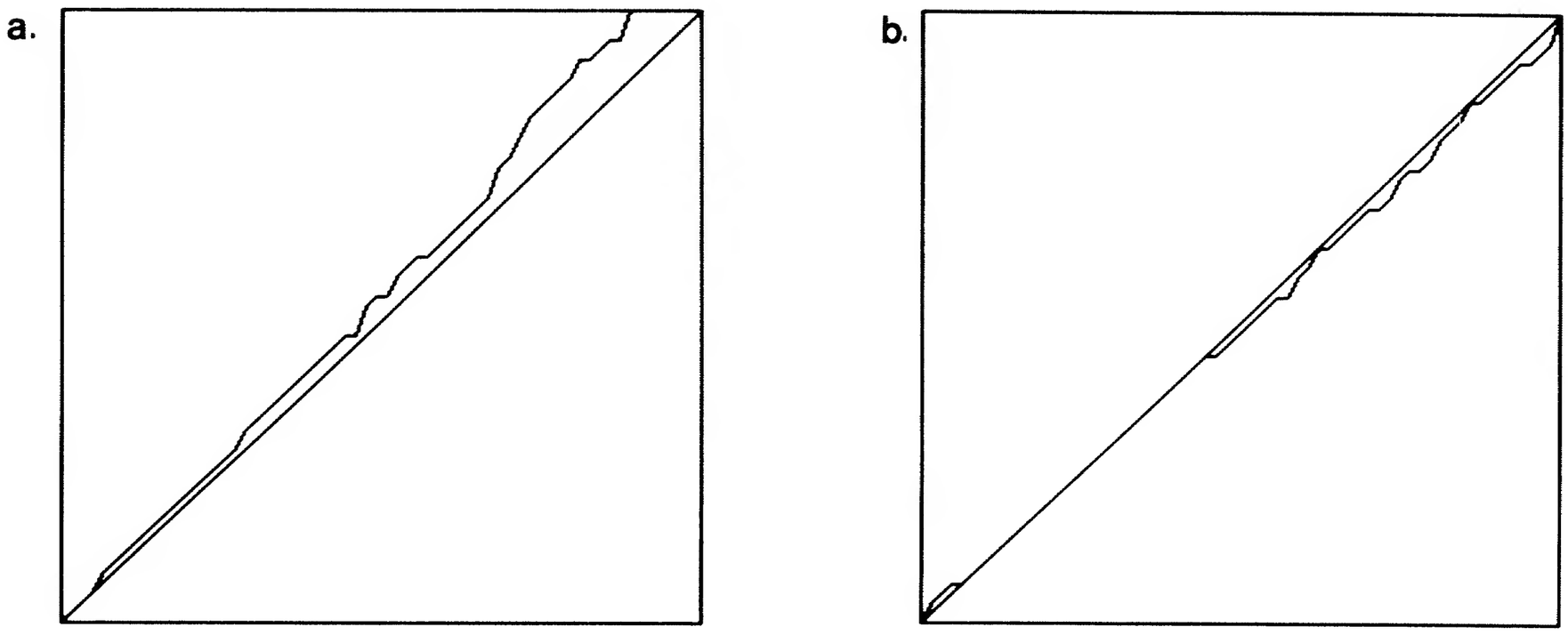

FIGURE 8